

Hydrostatic Pressure Compensator for Evaluation of Carotid Stiffness using A-Mode Ultrasound: Design, Characterization, and In-Vivo Validation

Ishwarya S
Healthcare Technology Innovation
Centre (HTIC), IIT Madras
Chennai, India
ishwarya.s@htic.iitm.ac.in

Rahul Manoj
Department of Electrical Engineering
Indian Institute of Technology Madras
Chennai, India
rahul_manoj@smail.iitm.ac.in

Raj Kiran V
Department of Electrical Engineering
Indian Institute of Technology Madras
Chennai, India
ee15d020@ee.iitm.ac.in

Nabeel PM
Healthcare Technology
Innovation Centre (HTIC), IIT Madras
Chennai, India
nabeel@htic.iitm.ac.in

Jayaraj Joseph
Department of Electrical Engineering
Indian Institute of Technology Madras
Chennai, India
jayaraj@ee.iitm.ac.in

Abstract—Arterial stiffness measured from central arteries is widely recognized as a prognostic marker for cardiovascular risk stratification. Measurements in sitting posture make stiffness assessment potentially more rapid and feasible for large-scale population-level field screening. However, the blood pressure (BP) required for stiffness evaluation must be compensated for any hydrostatic pressure offset while performing measurements in a sitting posture. In this work, we developed and validated a hydrostatic pressure compensation unit integrated with our A-mode ultrasound device for carotid artery stiffness. The system was characterized, and its design parameters were carefully considered for concurrence with a physiologically interesting range. The smallest change it could reliably measure was 2 mm, which corresponded to 0.3 mmHg of blood pressure. The device was validated on 20 human subjects (11 males and 9 females). The results demonstrated that the average carotid systolic and diastolic pressures compensated with the hydrostatic pressure were 29% and 22% lesser than those without compensation. The ANOVA showed a statistically significant difference ($p < 0.0001$) between the β obtained from compensated (5.21 ± 0.43) and uncompensated (5.73 ± 0.22) pressures. Whereas E_p , AC did not show a statistically significant difference as they rely on the pulse pressure, which was not affected by the hydrostatic pressure correction. Conclusively, hydrostatic pressure affects the stiffness markers that rely on the absolute pressure values.

Keywords—A-mode ultrasound, arterial stiffness, hydrostatic pressure, pulse pressure, stiffness markers, ultrasound.

I. INTRODUCTION

Arterial stiffness is a marker of vascular aging and cardiovascular events [1]. The age-related deterioration in the vascular structure and its functional impairment leads to the loss of elastic properties, especially in the central arteries such as the aorta and carotid from the earlier stage. Stiffening of the arteries would lead to hypertension [2], end-organ damage [3], coronary events, and stroke [4], exacerbating cardiovascular risks [5]. Early detection of arterial stiffness and timely intervention would provide better cardiovascular risk stratification. Given the importance of stiffness measurement and its prognostic value, large-scale screenings in the field and primary care units allow effective cardiovascular risk management. In either setting, for high

throughput screening and field usage, measurement in a sitting posture is preferable.

Commercial devices such as the SphygmoCor [6] and Pulsepen [7] are typically used to measure carotid-femoral pulse wave velocity (cf-PWV), regarded as the gold-standard measurement for arterial stiffness. These systems for regional stiffness measurement demand operator expertise and arterial path-length estimation over body surface [8]. Moreover, the operating protocols demand subjects to adopt a supine posture and expose the groin area when the tonometer is used for femoral pulse detection [8]. Local assessment of arterial stiffness, on the other hand, is performed on a single target arterial site such as the carotid artery or aorta (central arteries). Widely used local stiffness indices, namely, Specific stiffness index (β), Peterson elastic modulus (E_p), Arterial compliance (AC) [9], and local pulse wave velocity [10], are evaluated using arterial diameter and pressure with the help of established biophysical models [8]. Predominantly, arterial diameter values required for the local stiffness evaluation are obtained using ultrasound imaging. However, clinical ultrasound measurement does not include an integrated pressure measurement unit. As a result, required pressure values are typically measured using an oscillometric device from the brachial artery and entered into a local stiffness monitoring system or post-processing station.

It may be noted that accurate evaluation of local stiffness indices of an artery requires both the pressure and diameter obtained from the same segment. For instance, aforesaid local stiffness estimates are commonly obtained from the carotid artery and require the carotid pressure (along with diameter), which is practically challenging. Owing to the anatomical structure of the common carotid artery without bone underneath, the use of applanation tonometry is not recommended at the neck for carotid pressure measurement [11]. Another approach wherein a proxy of carotid pressure waveforms is calibrated to required pressure levels demands technical expertise to give optimal applanation to avoid blood pressure (BP) cushioning. As such, methods involving the scaling of arterial diameter to pressure with the help of linear/non-linear pressure-diameter models have gained widespread acceptance in research [12].

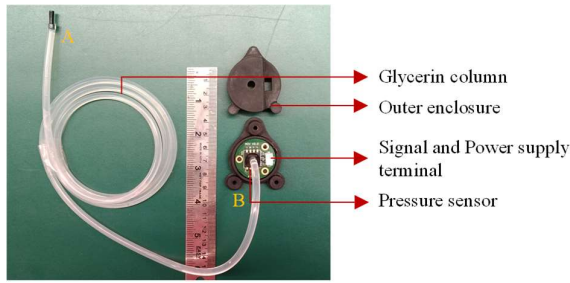


Fig. 1 Hydrostatic pressure compensation unit (HPCU).

Typically, the carotid artery pressure is obtained by scaling brachial BP through a carotid diameter waveform [12] under a rational assumption that the end-diastolic and mean arterial pressure are comparable throughout the arterial tree when the hydrostatic pressure offset between carotid and brachial sites are negligible. This is applicable, to a large extent, only when the subjects adopt supine posture at the time of measurement. However, measurements under the sitting posture are much more convenient and preferred for field measurement and high throughput screening. As such, pressure at the carotid artery experiences a significant hydrostatic pressure offset compared to brachial BP [13]. In the current devices that are used for local stiffness, the evaluation does not consider this effect. As a result, they can only perform measurements in a supine position [14] or be corrected for hydrostatic pressure externally when stiffness is assessed in sitting posture [15].

Addressing the need for inbuilt hydrostatic pressure compensation in local stiffness monitors, we have developed and validated a compact hydrostatic pressure compensation unit (HPCU) and integrated it into our clinically validated fully A-mode (image-free) ultrasound device ARTSENS[®] device [16][17]. The developed HPCU compensates for hydrostatic pressure at the carotid artery with respect to the heart level, and ARTSENS[®] performs the reliable evaluation of local stiffness markers even in sitting posture. In this work, we report the characterization of HPCU and demonstrate its functionality in yielding stiffness markers obtained from the carotid artery compensated for hydrostatic pressure offset.

II. MATERIALS AND METHODS

A. Principle of Hydrostatic Pressure Measurement

For a vertically arranged tube containing liquid, as shown in Fig. 1, the pressure at any given level within the tube is proportional to the height of the liquid column above it. The pressure is generally referred to as hydrostatic head or hydrostatic pressure (P_{hydro}) and is expressed as,

$$P_{\text{hydro}} = h\rho g + P_{\text{ref}} \quad (1)$$

Where h is the height of the measured site relative to P_{ref} that is measured using the liquid column, ρ is the density of the liquid, g is the acceleration due to gravity ($\sim 9.81 \text{ m/s}^2$), and P_{ref} is the reference pressure against which the hydrostatic pressure is measured. This allows a direct measurement of the hydrostatic pressure offset between any two points separated by a certain vertical distance. The available pressure sensors are either gauge, differential, or absolute types. Among these

sensors, a gauge-type forms a reliable choice for measuring such hydrostatic offsets as it provides a measurement relative to the local atmospheric pressure. Therefore, it accounts for the measurement variabilities potentially contributed by the change in altitude. The gauge pressure is expressed as,

$$P_m = P_{\text{hydro}} - P_{\text{atm}} = h\rho g + P_{\text{ref}} - P_{\text{atm}} \quad (2)$$

Where P_{atm} is the atmospheric pressure. When the tube is connected to the sensor on one end and exposed to the atmosphere on the other, P_m reduces to $h\rho g$, resulting in

$$h = \frac{P_m}{\rho g} \quad (3)$$

This arrangement can be potentially used while performing stiffness measurements from the carotid artery. While translating the brachial BP measurements to the carotid BP for the stiffness evaluation, any difference in the vertical level of the carotid site from the heart level introduces a hydrostatic offset. Measuring this level difference, employing the alluded principle and arrangement, enables compensation of the hydrostatic pressure offset. The developed HPCU in this regard is discussed as follows.

B. Design of Hydrostatic Pressure Compensator Unit

The HPCU comprises a non-compliant pressure tubing (ID: 4 mm, OD: 6 mm, tube length: 950 mm) filled with glycerine ($\rho = 1260 \text{ kg/m}^3$). The length of the tube was fixed based on the physiological range of distance measurement between brachial and carotid artery sites. One end of the tube (A) that is exposed to the atmosphere has a provision to be attached to the measurement probe (used for stiffness evaluation), and the other end (B) is connected to a pressure sensor module. The sensor with its integrated analog front end (AFE), the power supply regulation, and interfacing circuitries are secured in a custom 3D printed enclosure, as illustrated in Fig. 1. The exposed end of the tubing is plugged, leaving just a small orifice to avoid any seepage of the glycerine and yet be exposed to the atmosphere. Since end A is connected to the measurement probe, it moves with it, whereas end B is kept stationary at heart level.

The chosen pressure sensor (MP3V5010GC6U, NXP semiconductors, United States) provided an acceptable operational range -0 to 6.9 kPa , over an output voltage range of 0 to 3.3 V . It required a supply of 3.3 V , which it receives from the main power supply module of the ARTSENS[®] hardware it is integrated with. The sensor's analog output is digitized using a 12-bit low-speed analog-to-digital converter (ADC) of the ARTSENS[®] unit's microcontroller – (LPC4370FET256E ARM[®] Cortex[®]-M4 processor, NXP semiconductors). The ADC is configured to digitize the signals at a 250 Hz sampling rate to ensure synchronization with the ultrasound acquisitions.

C. Integration of HPCU with A-Mode Ultrasound Device

The ARTSENS[®] device is an A-mode (image-free) ultrasound device that is interfaced with a single channel ultrasound transducer (diameter = 5 mm , spatial half-angle $< 1.3^\circ$). The hardware primarily consists of a control unit, power supply unit, pulse-receiver, and high voltage unit responsible for operating the transducer in a pulse-echo

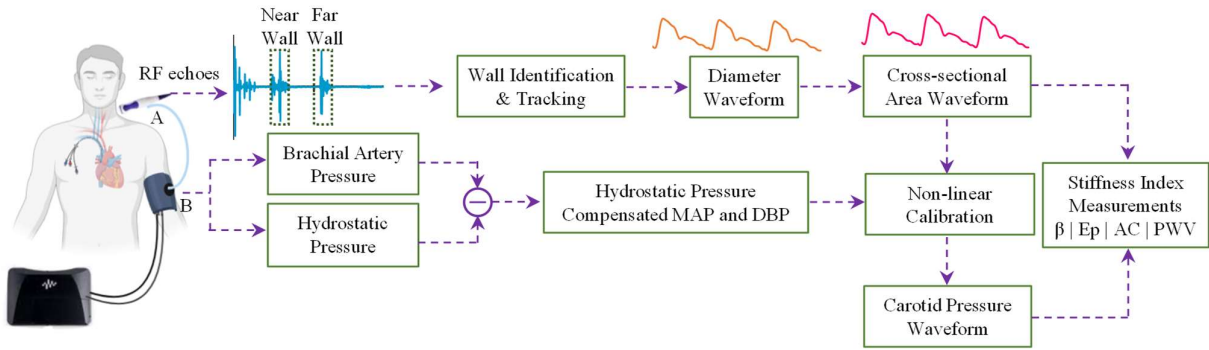


Fig. 2. The system architecture of Hydrostatic Pressure Compensation Unit integrated with an A-mode ultrasound device

mode. With the current configuration, the device performs the A mode scanning at a frame rate of 250 Hz and acquires the radio-frequency (RF) signals at a sampling rate of 80 MHz. This sampling rate ensures adequate resolution ($\sim 10 \mu\text{m}$) to track the continuous arterial wall locations. The recently evolved version of the technology also hosts an in-house developed oscillometric module for measuring brachial BP.

The HPCU's sensor circuitry, secured in the 3D printed enclosure, is interfaced with the A-mode device via coaxial-shielded cable. The interfacing includes power lines, analog input/output terminal, and control lines. Such an arrangement synchronizes the HPCU's acquisition with the rest of the modules. The brachial cuff used for the device is custom-designed to house the HPCU's sensor end. Therefore, the sensor unit is ensured stationary at the heart level during the measurement.

D. Calibration of HPCU

The HPCU digitized signals were initially acquired using the A-mode device hardware for calibration purposes. The acquired voltage signals were pre-processed using a moving average filter of 25 samples for denoising and then were used for calibration. The voltage signals were first calibrated for height measurements by recording the voltage levels while gradually increasing the height (steps of 50 mm starting from 0 to 950 mm) of the mobile end of the HPCU's tube. Linear regression was performed to identify the calibration parameters – slope and intercept.

E. Data Processing for Stiffness Evaluation

The computing software was developed on LabVIEW® (National Instruments, USA) for the automated evaluation of the stiffness parameters. During the measurement procedure, the computing software captures the digitized RF echoes and HPCU voltage signals simultaneously in real-time. The HPCU digitized signals are pre-processed and converted to the corresponding height measurements based on the input calibration parameters. The height measurements then are converted to the equivalent hydrostatic blood pressure using the density of blood as 1060 kg/m^3 .

The digitized RF echoes are filtered using a zero-phase 4th order bandpass filter (1 MHz to 10 MHz) and processed using extensively validated automated algorithms to yield diameter waveform [18][19]. These algorithms identify and continuously track the carotid artery's near and far wall locations by employing cross-correlation methods [20]. The

algorithm distinguishes between dynamic and static components of the signal and further distinguishes between oppositely moving echoes that are next to each other. As a result, the algorithm is sensitive to the presence or absence of the artery. The dynamic and static components are distinguished using cross correlation-based shift estimation methods, with the dynamic portions having a positive [20] or negative shift and the static portions having a zero shift. The diameter waveforms provide the beat-to-beat peak distension and end-diastolic diameter values [19].

Further, the carotid BP is also derived from the diameter waveforms for the individual cardiac cycles by adopting a technique to scale the brachial BP values [14] non-linearly. The hydrostatic offset obtained at 1000Hz is averaged for 100 samples and is used to correct the corresponding beat's carotid BP measurements. The stiffness markers (E_p , β , PWV, AC) are computed from the obtained carotid pressure, peak distension, and end-diastolic diameter values.

F. Experiments to characterize HPCU

The HPCU was characterized for resolution, hysteresis, and drift in calibration based on independent controlled

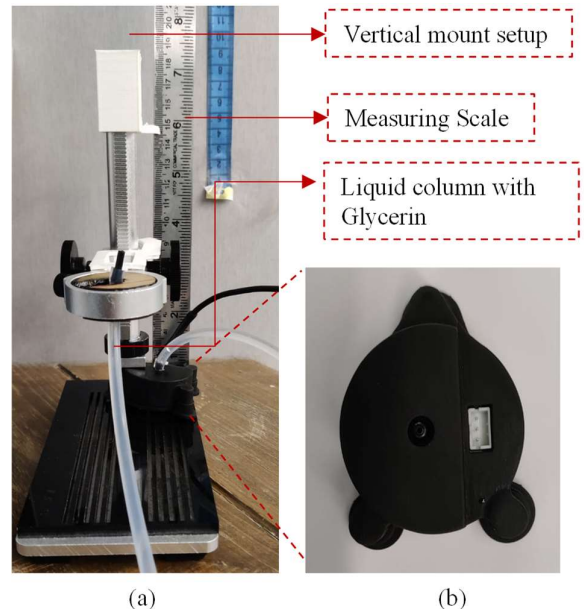


Fig. 3. (a) Experimental setup to determine the resolution of the system, (b) Hydrostatic Pressure Compensation Unit (HPCU).

TABLE I LOCAL STIFFNESS INDICES

| Stiffness Indices | Expression |
|--|---|
| Peterson Elastic Modulus, E_p (kPa) | $E_p = \frac{D_d \times \Delta P}{\Delta D}$ |
| Specific Stiffness Index, β | $\beta = \frac{\ln(P_s/P_d)}{(\Delta D/D_d)}$ |
| Arterial Compliance, AC (mm^2/kPa) | $AC = \frac{\pi(D_s^2 - D_d^2)}{4\Delta P}$ |

experiments post to the calibration procedure. Initially, the amplitude of the white noise was evaluated by recording the signals at a zero-height level, i.e., keeping both ends of the tube proximal to each other. For assessing its resolution, a dedicated setup was developed with a provision to increase the height with a resolution of 1 mm over a range of 30 to 50 mm (concerning the platform on which the sensor end of the tube was placed). The mobile end of the tube was mounted into a platform, as shown in Fig. 3, where the platform could be moved vertically using a gear mechanism. The voltages were recorded incrementing the level (30 to 50 mm) with different step sizes for each trial ranging from 5 mm to 1 mm. The step-resolvability was inspected for each trial to identify the resolution from the recorded signals. Further, for assessing the hysteresis of the HPCU, a loading-unloading protocol was followed where the voltage values were collected for different levels ranging from 0 to 950 mm with incrementing and decrementing by a step size of 50 mm. Finally, the reproducibility of the calibration was inspected by monitoring the drift in the voltage-to-height linear curve recorded over four weeks (once a week).

G. In-vivo Functionality Verification Study

An in-vivo study was conducted on twenty healthy human subjects aged 21 to 42 years (11 males, 9 females). The study was reviewed and approved by the Institute review boards of IIT Madras (IEC/2021-01/JJ/07). The participants were recruited opportunistically, and written informed consent was obtained prior to the study.

The anthropometric measurements were collected, and the subjects were allowed to rest for 5 to 10 mins in a sitting posture. The brachial cuff wrapped around the subject's left arm, and the sensor unit of the HPCU was attached to the cuff. The subject was asked to place their hand on the armrest of the chair comfortably. The brachial BP and heart rate were

measured using the A-mode ultrasound. The left carotid artery location was identified by palpation, and the ultrasound measurements were performed accordingly. For comparison purposes, the stiffness markers were derived from the recorded signals before and after introducing the hydrostatic pressure correction for the carotid BP estimates. The equations for the stiffness values are specified in Table I. Where ΔD represents the peak arterial distension, D_d is the end-diastolic diameter, and D_s is the systolic diameter. P_s and P_d are the systolic and diastolic pressures, respectively.

H. Statistical Analysis

All continuous variables were presented as mean \pm standard deviation. The pre and post hydrostatic pressure compensated stiffness estimates were compared and represented using box and whisker plots. The median and interquartile ranges are indicated in these box-whisker plots. ANOVA was used to show the statistical significance of any difference between the groups, presented using the p-value. A level of significance $\alpha = 0.05$ was used for all tests. A p-value < 0.05 rejected the null hypothesis and confirmed the statistical significance. The variabilities were indicated using the coefficient of variation (CoV) evaluated as the ratio of standard deviation to the mean of the measurements (expressed in %). All analyses were performed using SAS[®] OnDemand for Academics, and plots were constructed using Microsoft Excel (Version 19.0, USA).

III. RESULTS AND DISCUSSIONS

A. HPCU Characteristics

At zero height level, the noise in the voltage signal resulted in a height of 0.86 mm. Similarly, the standard deviation from its measured mean value was 0.87 ± 0.12 mm for the other height levels. This dictated the resolution offered by HPCU for height measurement.

The experiments revealed that height measurements were resolvable for step increments beyond 2 mm, which concurs with the standard deviation limits. This may be observed in Fig.4(a), which depicts the sample recordings performed during the 2 mm step-increment trial. The system, therefore, offered a corresponding resolution of 0.3 mmHg for the blood pressure measurement.

Since the recruited pressure sensor could measure pressure in the range of 0 to 6.9 kPa, a height of 0 to 950 mm and consequently a hydrostatic blood pressure of 0 to 51.75 mmHg was measurable. The HPCU was designed to measure

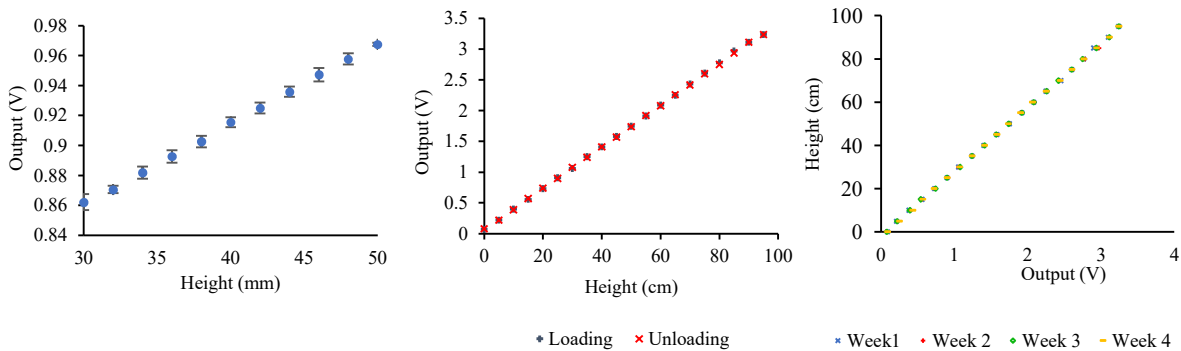


Fig. 4. Characterization of the Hydrostatic Pressure Compensation Unit; (a) Plot illustrating resolution of the system, (b) Loading and Unloading of the system, (c) Distribution of drift of calibration in 4 weeks.

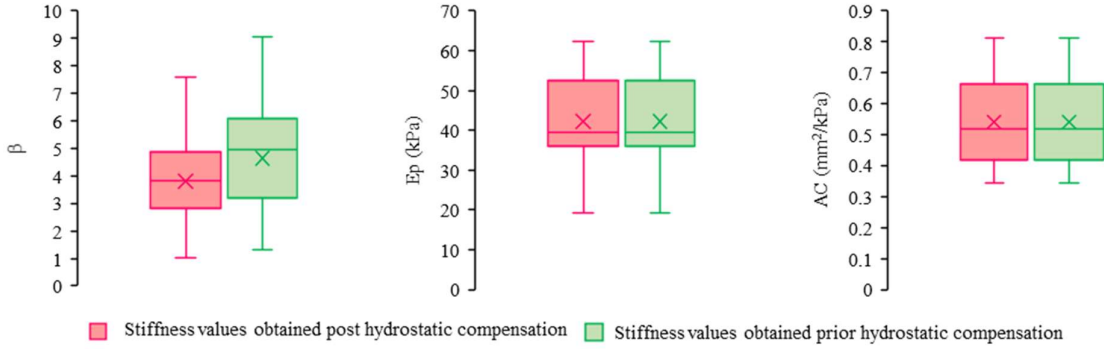


Fig. 5. Box and Whisker plots illustrating comparison of (a) β , (b) E_p and (c) AC with and without compensating for hydrostatic pressure.

a full-scale height of 950 mm (~ 51 mmHg), which is within the operational range of the sensor. The average distance between the carotid and heart for the recruited population was 260 ± 30.5 mm, which falls very well under the system's measurable range. The recorded voltage (in V) versus the reference height (in cm) exhibited a linear relationship ($h = 27.6 \times \text{sensor voltage} + 1.7$), resulting in a sensitivity of 3.9 mV/cm.

B. Calibration Reliability

Fig. 4(b) shows the effect of loading and unloading on the voltage-to-height relationship. It may be observed that incrementing and decrementing the vertical level had an identical effect on the output voltages of the HPCU. The mean difference between loading and unloading phase voltages was 0.006 ± 0.01 V, which was insignificant ($p = 0.99$). This manifested an absence of hysteresis and negligible nonlinearity. The calibration performed over four weekly trials was consistent with a CoV of 0.3% and 11% in the evaluated slopes and intercepts, indicating the robustness of HPCU towards measurement drifts. With the final calibration parameters (slope = 29.72 and intercept = 1.79), the absolute percentage error in the measured versus reference heights (over the range of 0 to 950 mm) was 8.8 ± 7.1 % (error = 8.7 ± 7.2 mm), and the variability in the measured heights over four trials was 2.3%. This demonstrated the HPCU's accuracy and repeatability, suggesting its reliability for stiffness evaluation.

C. Blood pressure and Stiffness Measurements

The descriptive characteristics for the recruited population are presented in Table II, enlisting the anthropometric, blood pressure, and stiffness measurements. The estimated carotid P_s was systematically smaller than brachial by 8.59 ± 4.49 mmHg. The pulse pressure amplification assessed by the device was concurrent with literature (range = 11 to 14 mmHg) [21]. The hydrostatic head in sitting posture further influences the carotid BP, which, as measured in this study, was 17.3 ± 4.5 mmHg. Thus, BP after hydrostatic compensation at the carotid artery showed a further reduction.

The box and whisker plots for the evaluated arterial stiffness parameters using the pre and post hydrostatic corrected carotid pressures are shown in Fig. 5. It is seen from the results that the β adjusted for hydrostatic pressure shows an underestimated value compared to the ones without the compensation ($p < 0.0001$). Similar On the other hand, the E_p

TABLE II DESCRIPTIVE STATISTICS

| Parameters | Number/ Mean \pm SD |
|--|-----------------------|
| Subjects (male/female) | 20 (11/9) |
| Age (Years) | 24 – 42 |
| Body mass index (kg/m^2) | 25.60 ± 4.28 |
| Brachial P_s (mmHg) | 112.5 ± 10.5 |
| Brachial P_d (mmHg) | 75.8 ± 8.1 |
| Carotid P_s (mmHg) without HP compensation | 103.9 ± 11.7 |
| Carotid P_d (mmHg) without HP compensation | 75.8 ± 8.1 |
| Carotid P_s (mmHg) with HP compensation | 87.2 ± 12.3 |
| Carotid P_d (mmHg) with HP compensation | 59.25 ± 9 |

and AC did not show any statistically significant difference between the hydrostatic compensated and uncompensated values. Contrary to β , the expressions for evaluating the E_p and AC include only a pulse pressure ($P_s - P_d$) term instead of the absolute values of P_s and P_d .

Therefore, since the hydrostatic offset corrections apply to the carotid P_s and P_d preserving the carotid pulse pressure, they were observed to affect only the stiffness markers directly relying on the absolute values of the pressures. The parameters like E_p and AC make use of only the pulsatile component ($P_s - P_d$) for their calculation and therefore any hydrostatic pressure that augments P_s and P_d is cancelled out during the calculation. Hence, they mask the effect of hydrostatic pressure change on the stiffness. However it may be noted that stiffness is a pressure dependent parameter the parameter must exist these pressure dependencies to standardize it [22]. Furthermore, when constructing a nomogram for a large demographic sample through clinical or field research, the posture of the measurement should be taken into account. Since these stiffness properties differ between supine and seated, it is necessary to account for the effect of hydrostatic pressures in order to standardize the measurement.

IV. CONCLUSION

This work has developed and characterized the HPCU integrated with the A-mode ultrasound device to measure hydrostatic pressure compensated stiffness indices. The developed system manifested reliable functionality. The resolution obtained (2 mm) was sufficient for the application. The system showed good linearity, and the effect of

hysteresis was also negligible. The repeatability and reproducibility of the measured values show the system's stability. The in-vivo study on 20 subjects was conducted in sitting posture. The stiffness indices (β , Ep, AC) were calculated from the carotid blood pressures prior to and post hydrostatic compensation. The study results illustrate an underestimation of 20% between the hydrostatic compensated and uncompensated stiffness indices that rely on the absolute pressures. In conclusion, a device like this would help evaluate the carotid stiffness markers that account for hydrostatic pressure gradient and allow reliable sitting measurements in the field and clinical setting, which are preferred due to the low resource-constrained settings [23]. This study addresses one crucial factor by measuring sitting posture, which may be required while measurements in clinical setup. This HPCU could also be an integral part of any wearable devices, cuffless BP measurements, and local PWV measurements.

V. REFERENCES

- [1] C. Vlachopoulos, K. Aznaouridis, and C. Stefanadis, "Prediction of Cardiovascular Events and All-Cause Mortality With Arterial Stiffness. A Systematic Review and Meta-Analysis," *J. Am. Coll. Cardiol.*, vol. 55, no. 13, pp. 1318–1327, 2010, doi: 10.1016/j.jacc.2009.10.061.
- [2] Safar ME and O'Rourke ME, *Arterial stiffness in hypertension, 2006. In Handbook of hypertension, vol 23*, Elsevier, 2006.
- [3] R. R. Townsend *et al.*, *Recommendations for Improving and Standardizing Vascular Research on Arterial Stiffness: A Scientific Statement from the American Heart Association*, vol. 66, no. 3, 2015.
- [4] A. K. Chomistek *et al.*, "Relationship of sedentary behavior and physical activity to incident cardiovascular disease: Results from the women's health initiative," *J. Am. Coll. Cardiol.*, vol. 61, no. 23, pp. 2346–2354, 2013, doi: 10.1016/j.jacc.2013.03.031.
- [5] D. K. Arnett, G. W. Evans, and W. A. Riley, "Arterial stiffness: A new cardiovascular risk factor?," *Am. J. Epidemiol.*, vol. 140, no. 8, pp. 669–682, 1994, doi: 10.1093/oxfordjournals.aje.a117315.
- [6] M. W. Rajzer, W. Wojciechowska, M. Klocek, I. Palka, M. Brzozowska-Kiszka, and K. Kawecka-Jaszcz, "Comparison of aortic pulse wave velocity measured by three techniques: Complior, SphygmoCor and Arteriograph," *J. Hypertens.*, vol. 26, no. 10, pp. 2001–2007, 2008, doi: 10.1097/HJH.0b013e32830a4a25.
- [7] T. Pereira, C. Correia, and J. Cardoso, "Novel methods for pulse wave velocity measurement," *J. Med. Biol. Eng.*, vol. 35, no. 5, pp. 555–565, 2015, doi: 10.1007/s40846-015-0086-8.
- [8] P. M. Nabeel, V. R. Kiran, J. Joseph, V. V. Abhidev, and M. Sivaprakasam, "Local Pulse Wave Velocity: Theory, Methods, Advancements, and Clinical Applications," *IEEE Rev. Biomed. Eng.*, vol. 13, pp. 74–112, 2020, doi: 10.1109/RBME.2019.2931587.
- [9] A. K. Sahani, J. Joseph, and M. Sivaprakasam, "Automated system for imageless evaluation of arterial compliance," *Proc. Annu. Int. Conf. IEEE Eng. Med. Biol. Soc. EMBS*, pp. 227–231, 2012, doi: 10.1109/EMBC.2012.6345911.
- [10] P. M. Nabeel, J. Joseph, and M. Sivaprakasam, "A Magnetic Plethysmograph Probe for Local Pulse Wave Velocity Measurement," *IEEE Trans. Biomed. Circuits Syst.*, vol. 11, no. 5, pp. 1065–1076, 2017, doi: 10.1109/TBCAS.2017.2733622.
- [11] M. F. O. Rourke, "Carotid Artery Tonometry : Pros and Cons," pp. 15–17, 2015, doi: 10.1093/ajh/hpv194.
- [12] J. M. Meinders and A. P. G. Hoeks, "Simultaneous assessment of diameter and pressure waveforms in the carotid artery," *Ultrasound Med. Biol.*, vol. 30, no. 2, pp. 147–154, 2004, doi: 10.1016/j.ultrasmedbio.2003.10.014.
- [13] R. Mukkamala, J. Hahn, and O. T. Inan, "Towards Ubiquitous Blood Pressure Monitoring via Pulse Transit Time : Theory and Practice," vol. 9294, no. c, 2015, doi: 10.1109/TBME.2015.2441951.
- [14] E. C. Schroeder, A. J. Rosenberg, T. I. M. Hilgenkamp, D. W. White, T. Baynard, and B. Fernhall, "Effect of upper body position on arterial stiffness: Influence of hydrostatic pressure and autonomic function," *J. Hypertens.*, vol. 35, no. 12, pp. 2454–2461, Dec. 2017, doi: 10.1097/HJH.0000000000001481.
- [15] P. M. Nabeel, J. Joseph, S. Karthik, M. Sivaprakasam, and M. Chenniappan, "Bi-Modal arterial compliance probe for calibration-free cuffless blood pressure estimation," *IEEE Trans. Biomed. Eng.*, vol. 65, no. 11, pp. 2392–2404, 2018, doi: 10.1109/TBME.2018.2866332.
- [16] P. M. Nabeel *et al.*, "An image-free ultrasound device for simultaneous measurement of local and regional arterial stiffness indices," *2021 IEEE Int. Symp. Med. Meas. Appl. MeMeA 2021 - Conf. Proc.*, pp. 1–6, 2021, doi: 10.1109/MeMeA52024.2021.9478737.
- [17] J. Joseph, P. M. Nabeel, S. R. Rao, R. Venkatachalam, M. I. Shah, and P. Kaur, "Assessment of Carotid Arterial Stiffness in Community Settings with ARTSENS®," *IEEE J. Transl. Eng. Heal. Med.*, vol. 9, no. November 2020, 2021, doi: 10.1109/JTEHM.2020.3042386.
- [18] K. V. Raj, J. Joseph, N. P. M., and M. Sivaprakasam, "Automated measurement of compression-decompression in arterial diameter and wall thickness by image-free ultrasound," *Comput. Methods Programs Biomed.*, vol. 194, p. 105557, 2020, doi: 10.1016/j.cmpb.2020.105557.
- [19] A. K. Sahani, J. Joseph, R. Radhakrishnan, and M. Sivaprakasam, "Automatic measurement of end-diastolic arterial lumen diameter in ARTSENS," *J. Med. Devices, Trans. ASME*, vol. 9, no. 4, pp. 1–11, 2015, doi: 10.1115/1.4030873.
- [20] J. Joseph *et al.*, "ARTSENS(®) Pen-portable easy-to-use device for carotid stiffness measurement: technology validation and clinical-utility assessment," *Biomed. Phys. Eng. express*, vol. 6, no. 2, p. 25013, Feb. 2020, doi: 10.1088/2057-1976/ab74ff.
- [21] M. E. Safar and A. Kakou, "Carotid and brachial blood pressure measurements in hypertensive subjects," 2008.
- [22] P. M. Nabeel, J. Joseph, and M. Sivaprakasam, "Variation in local pulse wave velocity over the cardiac cycle: in-vivo validation using dual-MPG arterial compliance probe," *13th Russ. Conf. Biomed. Eng.*, no. June, pp. 100–103, 2018, [Online]. Available: <https://publications.rwth-aachen.de/record/723594>.
- [23] J. Nürnberger, R. Michalski, T. R. Türk, A. O. Saez, O. Witzke, and A. Kribben, "Can arterial stiffness parameters be measured in the sitting position," *Hypertens. Res.*, vol. 34, no. 2, pp. 202–208, Feb. 2011, doi: 10.1038/hr.2010.196.